2014

Bio-based soft elastomeric capacitor for structural health monitoring applications

Sari Kharroub
Iowa State University

Bio-based soft elastomeric capacitor for structural health monitoring applications

by

Sari Kharroub

A thesis submitted to the graduate faculty

in partial fulfillment of the requirements for the degree of

MASTER OF SCIENCE

Major: Civil Engineering

Program of Study Committee:
Simon Laflamme, Major Professor
Samy Madbouly
Jay Shen

Iowa State University

Ames, Iowa

2014

TABLE OF CONTENTS

LIST OF FIGURES

LIST OF TABLES

ACKNOWLEDGEMENTS

The project would not have been possible without the support of many people. Many Thanks to my advisor, Dr. Simon Laflamme, who provided continual support and guidance in all times of research and writing of this thesis. I could not have imagined having a better advisor and mentor for my Master's study.

Besides my advisor, I would like to thank Dr. Samy Madbouly and Dr. Jay Shen who gave their time and helpful direction as members of the thesis committee.

I thank my fellow group and office mates Hussam Saleem, Andrew Sundal, Matthew Schmitt, Adam Miller, Austin Downey, and Liang Cao for the simulating discussions, willingness to help, entertainment, and caring they provided.

I also thank the Iowa Energy center (grant 13-02) and the Iowa Alliance for Wind Innovation (grant 1001062565) for supporting this work.

Last but not least, I cannot finish without thanking my family. I warmly thank my parents Jrasmus and Naila Kharroub, and my siblings for always being there to support and encourage me in every aspect of life.

ABSTRACT

Large-area electronics are typically fabricated from petroleum-based polymers. However, petroleum has negative impacts on the environment and is expected to last for only another 80 years. Much attention, as a result, has been brought to minimize the usage of petroleum-based products and move towards environmental friendly products. This thesis presents a bio-based soft elastic capacitor (SEC), which is flexible and mainly made of water and vegetable oil. The SEC is composed of dielectric sandwiched between two electrode layers and it is used in structural health monitoring applications. The linearity of the sensor and its ability to transduce local strain of large surfaces into change in capacitance is demonstrated in this work. Additionally, the materials properties was tested and good physical and chemical properties are shown despite a decay of the dielectric that occurs after the first 16 days of fabrication.

CHAPTER 1

INTRODUCTION

Different types of structures, whether they are new or old, may have had or will possibly have deficiencies that cannot be identified unless a disaster is experienced. However, economic and human losses at that point are significant. The number of causalities and costs can even significantly increase when damages occur to critical and large public gathering buildings including hospitals, schools, and sports arena. As a result, it is necessary to conduct conditional assessment on all structures in order to improve safety and reduce costs as well as enhance maintenance and schedule programs.

1.1 Problem Statement

There are many available techniques and methods available to monitor structures including visual inspection, non-destructive evaluations, and most recently sensing system technologies. For sensors, polymers have been receiving growing attention by researchers as a new promising material. Polymer-based sensors are suitable for structural health monitoring applications due to their high accuracy and sensitivity, and short response time. The problem with the most commercially available polymers, however, is that they are derived entirely from non-renewable materials and produced from petroleum-based products (Madbouly, 2013) (Xia, 2010). Petroleum is a useful chemical substance for many important purposes but it is also a non-renewable resource with a highly toxic composition to many organisms, including humans. These toxins disturb large amounts of populated areas and ecosystem around the globe. In addition, crude oil prices are increasing and they are expected to last for only 80

more years (Chiellini, 2006). As a result, there is an urgent need to find environmentally-friendly, abundant, inexpensive, and renewable products to replace fossil feedstock and ensure sustainable development of sensors in structural health monitoring applications in the future.

1.2 Proposed Technology

This thesis proposes a soft elastic capacitor (SEC) made from bio-based materials that can be applied at large scales to measure local and global strain. The sensor is adhered to a structural element and change in strain of the monitored element causes a measurable change in capacitance of the sensor. The sensor is mainly made of water and vegetable oil, which are abundant and inexpensive. Thus, making the fabrication of the sensor much less costly and sustainable in the future.

The bio-based SEC has been developed as a possible replacement to a petroleum-based SEC previously developed by Laflamme *et al* (Laflamme, 2012), (Laflamme, 2013), fabricated from a styrene-ethylene/butylene-styrene (SEBS) matrix. It was shown that such sensor combines the advantages of large area applications, flexibility, and robustness, which result in high scalability (Laflamme, 2012), (Laflamme, 2013).

1.3 Thesis Layout

This thesis is organized as follows:

In Chapter 1, the background of structural health monitoring and the advantages of bio-based materials in comparison with petroleum-based materials are described. The mechanism of the proposed SEC is also introduced.

In chapter 2, a review of the available sensors in structural health monitoring applications is

presented along with the background of the vegetable oil-based waterborne polyurethane.

In chapter 3, the background of the sensor is described, which includes a description of the material used, sensor fabrication process, sensing principle, and sensor applications.

In chapter 4, the description of the SEC on a materials perspective, with a discussion on the dispersion of the filler and decay of the dielectric is presented. Afterwards, the sensor's linearity is experimentally verified and its theoretical gauge factor is validated.

In chapter 5, the thesis is concluded.

CHAPTER 2

STATE-OF-THE-ART

This chapter is a short version of the work published in the Structural Health Monitoring journal by the author (Kharroub, 2014).

2.1 Introduction to Structural Health Monitoring

Structural Health Monitoring (SHM) is the automated process of structural condition assessment, aimed at replacing ineffective and judgment-dependent visual inspections. It is also considered as an improvement with respect to non-destructive evaluation techniques (Blitz, 1996) (Grosse, 2008), which are expensive and require highly-trained inspectors (Rens, 1997). Popular real-time SHM techniques include fiber-optics (Li, 2004)(Lopez, 2011)(Glisic, 2012) and piezoelectric (giurgiutiu, 2007) sensors, which have shown capability of damage diagnosis, but typically require embedment. Surface sensing strategies such as accelerometers (Da, 2009) are less expensive to install, but result in a more complex signal processing task that makes damage localization difficult. An alternative is the installation of large-area electronics (LAEs), which have the potential to detect local damages over a large surface by mimicking the biological function of skin (Laflamme, 2012)(Hurlebaus, 2004)(Carlson, 2006)(Tata, 2009)(Lipomi, 2011)(Hu, 2014)(Zhou, 2011).

2.2 Large-Area Electronics (LAEs)

LAEs are enabled by recent advances in conductive polymers (Gangopadhyay, 2000). Popular applications in SHM include the utilization of carbon nanotube (CNT) nanocomposites

to create resistive strain sensors (Loh, 2009)(Gao, 2010). CNT is typically used due to its strength and super-elastic attribute (Kang, 2006), but its utilization results in high fabrication costs and difficult scalability. Capacitance-based strain sensors have been proposed for various applications including strain (Arshak, 2000)(Suster, 2006), pressure (Lipomi, 2011), tri-axial force (Dobrzynska, 2013), and humidity (Harrey, 2002)(Hong, 2012) sensing. The vast majority of the applications utilize petroleum-based polymers (Madbouly, 2013) (Xia, 2010). However, with the rapidly growing markets of flexible electronics and sensors, there is an economic and social pressure to utilize environmentally-friendly materials to support large-scale deployments.

2.3 Environmentally-Friendly Material

With the exception of castor oil, nearly all vegetable oils do not naturally have the hydroxyl groups necessary to produce polyurethane dispersions (PUDs). The carbon-carbon double bonds and the ester functionality present in triglycerides allow for the introduction of such groups, a technique leveraged in the production of the majority of the vegetable oil-based polyols. The proposed sensor is a bio-based LAE soft elastomeric capacitor, and its dielectric is constituted from a castor oil-based polyurethane (PU) mixed with titanium dioxide (TiO_2 or titania) particles. Vegetable oil-based waterborne polyurethane has recently emerged as a new branch of PU chemistry in an effort to reduce negative impacts on the environment and minimize fabrication costs. This branch has been rapidly growing, driven by the versatility and environmental friendliness of these PUs. Here, waterborne castor oil-based PUD is used in order to partly eliminate organic solvents in the SEC's fabrication process (Madbouly, 2013) (Lu, 2008) (Lu, 2005). This results in the reduction of toxic volatile organic compounds that exist in conventional PUs in significant amounts, and minimization of hazardous air pollutants (Lu,

2008). Unlike solvent-based PUDs, the aqueous PUDs can be applied with high solids content, because their viscosity does not depend on the molecular weight of polyurethane.

CHAPTER 3

BACKGROUND

This chapter is a short version of the work published in the Structural Health Monitoring journal by the author (Kharroub, 2014).

3.1 Materials

Castor oil, isophorone diisocyanate (IPDI), dimethylol propionic acid (DMPA), and dibutyltin dilaurate (DBTDL) were obtained from Aldrich Chemical Company (Milwaukee, WI). Methyl ethyl ketone (MEK) and triethylamine (TEA) were purchased from Fisher Scientific Company (Fair Lawn, NJ). SEBS was acquired from VTC Elastoteknik AB, Sweden, carbon black Printex XE 2-B from Orion Engineered Carbons (Kingwood, TX), and TiO_2 was purchased from Sachteleben Chemie GmbH (Germany). All materials were used as received without further purification or analysis.

Details about the synthesis of castor oil-based PUD can be found in a recent publication (Madbouly, 2013). Briefly, the castor oil-based PUD are synthesized by a reaction of IPDI, castor oil, and DMPA as internal surfactant. The DMPA incorporates carboxylic functionality in the prepolymer backbone. Tertiary amine (e.g., triethylamine, TEA) is then used to neutralize the carboxylic groups and produce ionic centres to stabilize the polymer particles in water.

TiO_2 is then dispersed in the castor oil in order to increase the permittivity of the PU. TiO_2 is considered as an environmentally-friendly inorganic material (Yang, 2013). The preparation of SEC is finalized by sandwiching the dielectric with two conductive electrodes fabricated from a carbon black and SEBS mix. Figure 1 illustrates the composition of a bio-based SEC.

Figure 1. A single bio-based SEC

3.2 Sensor Fabrication

The sensor's fabrication process is shown in Figure 2. Firstly, the dielectric of the capacitor (castor oil doped with TiO_2) is prepared using a solution casting method. TiO_2 nanoparticles are dissolved using methanol solvent before they are added to the castor oil PU at various volume percentages (5%, 10% and 15%) and dispersed using sonication with an ultrasonic tip. The resulting homogenous solution is drop-casted onto a glass plate and dried at room temperature for about 3 days to allow evaporation of water. Secondly, a 15 ml of SEBS/toluene solution is added to 0.79 g of carbon black to create the compliant electrodes. A sonication bath (Branson CPXH 2800) is used to disperse the carbon black particles. Finally, the carbon black-SEBS solution is sprayed on both surfaces of the dried polymer to form the sensor. The typical thickness of the resulting sensor is approximately 400 µm for the dielectric and 100

µm per electrode. Two conductive copper tapes are attached to the electrodes during the drying process to create mechanical connections for connecting to the data acquisition system (DAQ).

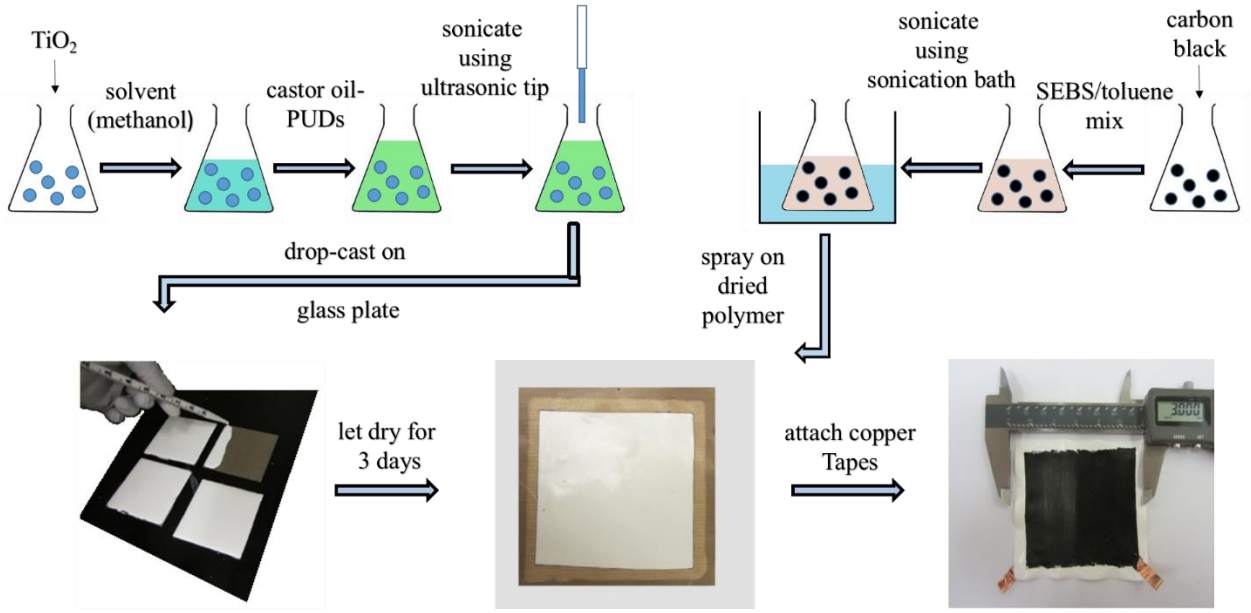

Figure 2. Sensor Fabrication

3.3 Electromechanical Model

The sensor behaves as a non-lossy capacitor when operating at relatively low frequencies (≤ 1kHz):

$$C = \frac{e_0 e_r A}{h} \tag{1}$$

where $A = w.l$ is the surface area of electrodes with width w and length l, and h is the thickness of the dielectric, e_0 =8.854 pF/m is the vacuum permittivity and e_r is the dimensionless relative

permittivity of the composite. Assuming small deformation, we can take the derivative of equation (1) to obtain the following expression:

$$\Delta C = \left(\frac{\Delta l}{l} + \frac{\Delta w}{w} - \frac{\Delta h}{h}\right) C \tag{2}$$

$$\frac{\Delta C}{C} = \epsilon_X + \epsilon_Y - \epsilon_Z \tag{3}$$

where ϵ is the strain in the principal axes illustrated in Figure 3. The SEC is designed to be adhered onto the surface of the monitored structure in the x-y plane using an epoxy. Taking Hooke's Law specialized for plane stress, we obtain an expression for ϵ_Z :

$$\epsilon_Z = -\frac{\nu}{1-\nu}(\epsilon_X + \epsilon_Y) \tag{4}$$

where ν is the Poisson's ratio of the sensor. Substituting equation (4) into equation (3) gives:

$$\frac{\Delta C}{C} = \lambda(\epsilon_X + \epsilon_Y) = \frac{1}{1-\nu}(\epsilon_X + \epsilon_Y) \tag{5}$$

where λ represents the gauge factor. Equation (5) can be rearranged using equation (1) to obtain the sensor's sensitivity:

$$\Delta C = \frac{\lambda(\epsilon_X + \epsilon_Y) e_0 e_r A}{h} \tag{6}$$

Equation (6) shows that the sensor's sensitivity in term of measured strain can be increased by increasing the width and length of the sensor, decreasing the thickness of dielectric or increasing the permittivity. In addition, equation (5) can be specialized for uniaxial strain along the *x*-axis of a monitored material of significantly higher stiffness (e.g., monitoring of a concrete beam). In this case, strain in the *y*-axis is written as $\epsilon_Y = -\nu_m \epsilon_X$, where ν_m is the Poisson's ratio of the monitored material. In this case, equation (5) becomes:

$$\frac{\Delta C}{C} = \lambda \epsilon_x = \frac{1-\nu_m}{1-\nu} \epsilon_x \tag{7}$$

Figure 3 illustrates the sensing of the SEC.

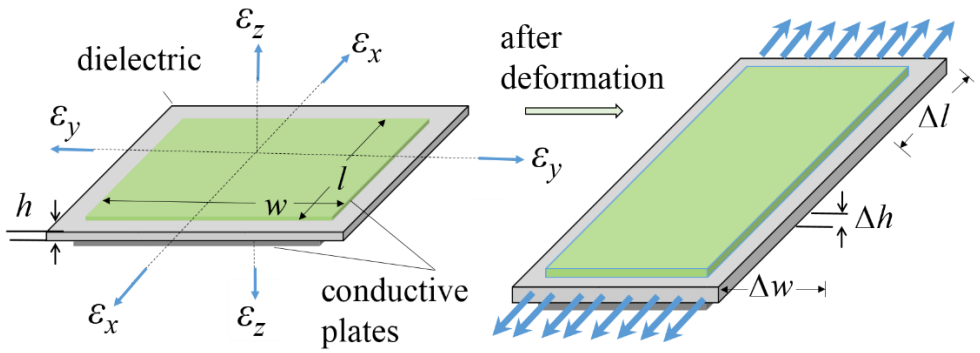

Figure 3. Sensing principle

3.4 Sensor Application

The bio-based SEC can be deployed in a large network configuration to cover and monitor surface strain over mesosurfaces. The sensor can be adhered to the structural element using an off-the-shelf epoxy. Measurements from the SEC can be used to diagnose and locate damage, and reconstruct physics-based features for condition assessment. In prior work on the

SEBSbased SEC of size similar to the bio-based SEC presented in this paper, the authors have demonstrated the utilization of four SECs deployed in a linear configuration to reconstruct deflection shapes (Laflamme, 2013). Example of possible applications include detection and localization of fatigue cracks on steel girders and condition assessment of wind turbine blades.

CHAPTER 4

EXPERIMENTAL INVESTIGATION

This chapter is a short version of the work published in the Structural Health Monitoring journal by the author (Kharroub, 2014). The tests in this chapter are conducted using SECs that are composed of TiO_2 as a dielectric sandwiched between two layers of carbon black and SEBS mix.

4.1 Material Properties

4.1.1 Dispersion of filler

Morphological inspection of the castor oil-based PU/TiO_2 nanocomposites was performed using scanning electron microscopy (SEM) for different TiO_2 contents. The samples were fractured in liquid nitrogen, fixed on the SEM holders, and sputtered with gold. The prepared samples were investigated using a field-emission scanning electron microscope (FE-SEM, FEI Quanta 250) operating at 10 kV under high vacuum. Figure 4 shows typical SEM micrographs for PU/TiO_2 nanocomposites with 5, 10, and 15 volume% TiO_2 to polymer contents, taken 3 days after fabrication. Prior experience using a petroleum-based polymer matrix showed that 20 volume% led to non-uniform dispersion due to a possible saturation of the filler (Laflamme, 2012). TiO_2 is dispersed along the horizontal axis, but appears to have settled in the vertical axis. A more uniform dispersion could be obtained by adding a coupling agent in the dielectric mix (Saleem, 2014), but such additive would introduce non-environmentally friendly chemicals in the process. Other fabrication methods, such as spin coating, could also be

considered. Given the utilization of the sensor in an in-plane mode, uniform dispersion is only required along the horizontal axis, yet preferable among the entire volume. The section on laboratory verification will confirm the homogeneous in-plane dispersion of the particles by demonstrating the linearity of the sensor and verifying the theoretical gauge factor experimentally. However, the non-uniform settlement along the sensor's thickness needs further investigation. Figure 5 shows a blow up on the region where TiO_2 has settled. The micrograph shows well dispersed TiO_2 in the PU matrix with an average particle size as small as 200 nm in this region.

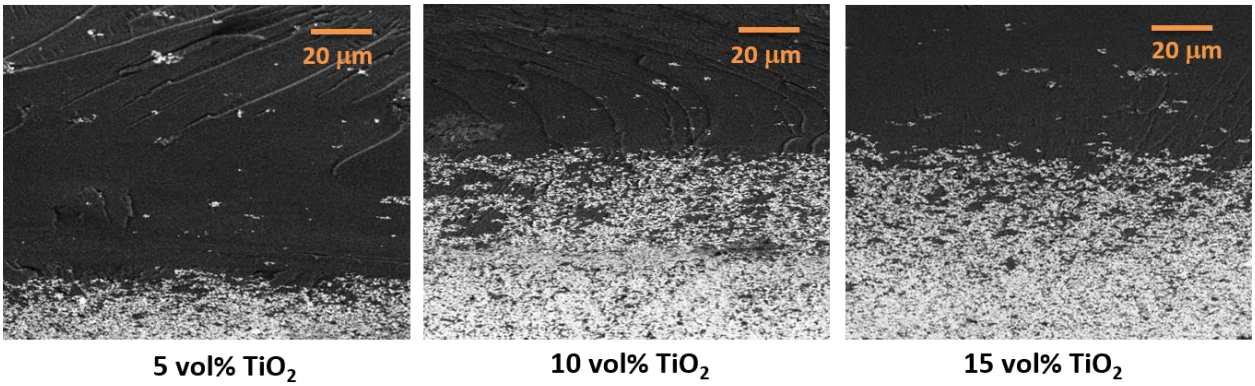

Figure 4. SEM micrographs for PU/TiO_2 nanocomposites for different composition

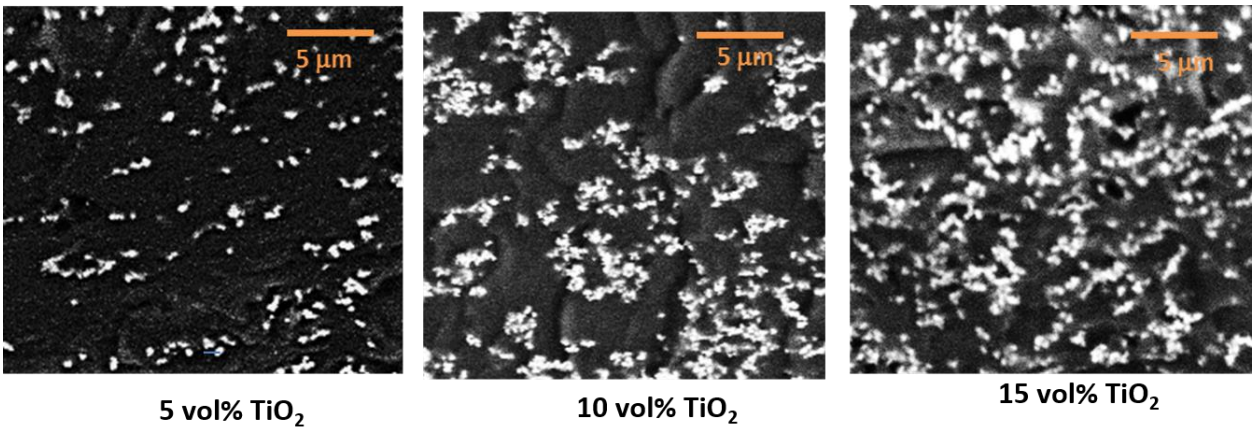

Figure 5. SEM micrographs for PU/TiO2 nanocomposites for different composition, blow up on dispersed titania particles.

4.1.2 Dielectric Properties

Experience with the castor oil-based SECs led to believe that a decay in the materials' dielectric occurred over time, phenomenon never observed with SEBS-based SECs. The change in the relative permittivity have been studied over time by recording the value of e_r over 3 weeks, by measuring the sensor's capacitance and back-calculating e_r using equation (1). Figure 6 is a plot of the average value of relative permittivity for each set of specimens (no recording was taken for the 9th and 10th days). The decay of the dielectric value is evident, and stabilizes after approximately 16 days. Possible explanations include slow evaporation of the soluble materials and reorganization of the filler. All tests discussed in this paper were performed on specimens older than 21 days to ensure a stable relative permittivity.

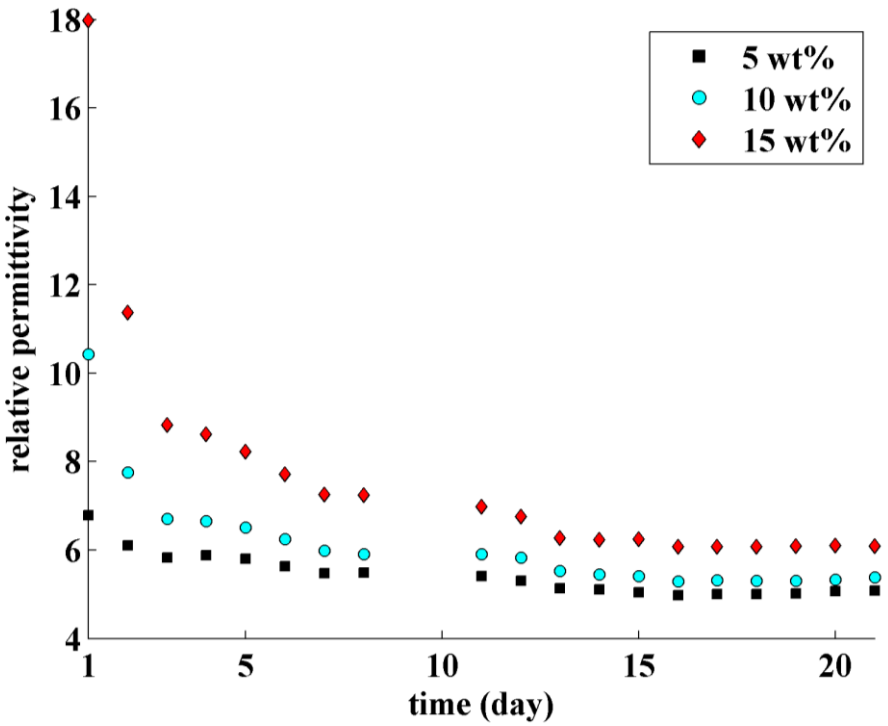

Figure 6. Average value of relative permittivity for each set over time

4.1.3 Thermogravimetric Analysis

The thermal stability of PU/TiO_2 nanocomposites was investigated using thermogravimetric analysis (TGA, model Q50 from TA Instruments, New Castle, DE) over a temperature range of 30°C up to 700°C at 20°C/min under nitrogen atmosphere. Figure 7 shows a typical TGA measurement for PU/TiO_2 nanocomposites for different TiO_2 contents. Results show that the pure PU sample is thermally stable at a temperature range up to 250°C. Approximately 10 wt% of the sample is degraded at approximately 250–300°C. This process is related to the evaporation of soluble materials and unreacted oil fragments. With increasing the temperature up to 600 °C, two fast degradation processes were observed. The first one at the temperature range of 300–380 °C, where approximately 60 wt% of the sample was lost due to the

degradation of the polymer backbone. The second process at approximately 400–600 ºC could be caused by further decomposition of the PU fragments. The multiple thermal degradation processes of bio-based polymers from vegetable oils are very common in literature. The thermal stability of these multiple degradation processes increased significantly (i.e., shifted to higher temperature ranges) by adding TiO_2 as seen in Figure 7. TiO_2 increases both the dielectric permittivity and the thermal stability of castor oil-based PU.

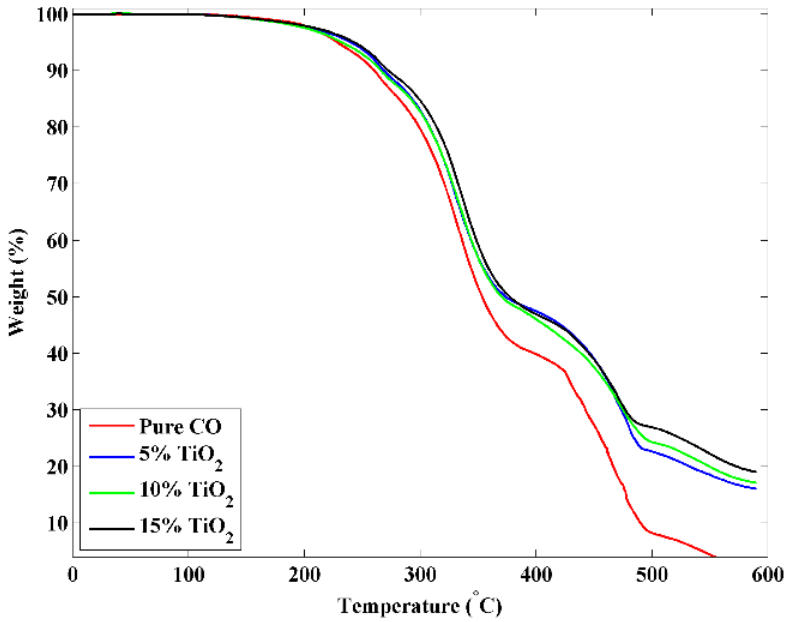

Figure 7. TGA measurements for PU/TiO_2 composites at 20ºC/min heating rate under nitrogen atmosphere.

4.2 Laboratory Verification

4.2.1 Experimental Setup

A free-standing sensor and a bending beam tests were conducted to validate the linearity of the proposed SEC over the range 0-6% strain, and verified the gauge factor (equation (7)) by deploying the sensor on a simply supported beam subjected to bending.

Free Standing sensor test

In the free-standing sensor test, three SEC with 5, 10, and 15 TiO_2 volume% were clamped separately into an Instron table-top mechanical testing machine (model 5569). Each of the sensor was subjected to six tensile strain cycles (from 1% to 6% strain with 1% strain increment), with each strain plateau attained at a loading rate of 5mm/min. This range of strain was governed by the allowable elongation of the testing equipment for the sample sizes, and is well beyond the failure point of typical structural materials. Data from the SECs were acquired using ACAM PCap01 sampled at 95.8 Hz . Figure 8 shows the laboratory setup for the free-standing sensor test. It is worth noting that equation (7) cannot be verified in a free-standing configuration because of the non-uniform distribution of strain within the dielectric.

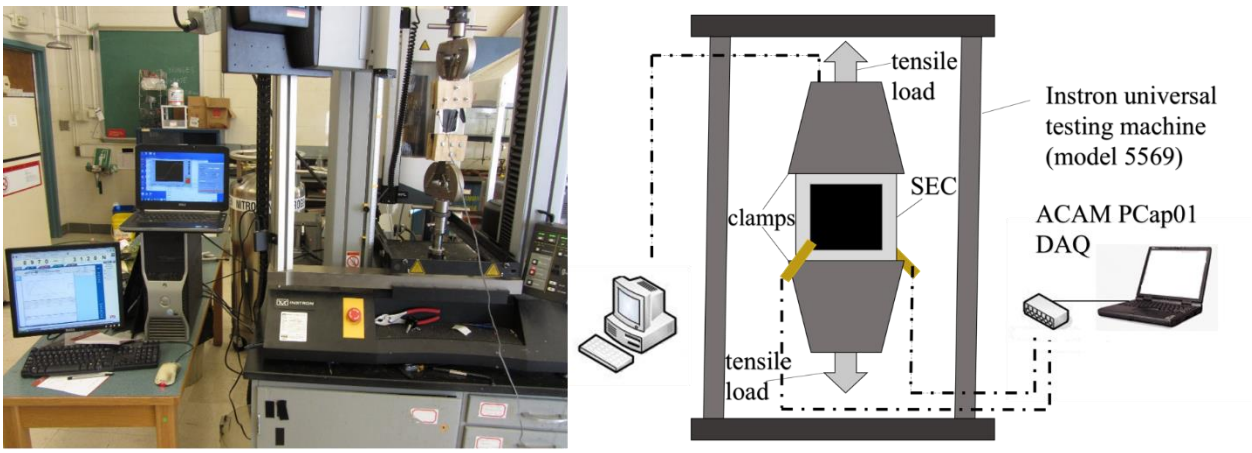

Figure 8. (a). Tensile test laboratory setup; (b) schematic of the clamped SEC on the Instron machine

Bending Beam test

In the bending beam test, the SEC specimens were installed onto the bottom surface of a simply supported aluminium plate of dimensions (36 x 8 x 0.25 in^3) subjected to a four-point load setup as shown in figure 9. Each sensor was deployed within the uniform moment region using a thin layer of an off-the-shelf epoxy (JB Kwik) after sanding the plate surface and applying a primer. Step loads (approximately 20 lb., 40 lb., 60 lb., and 80 lb.) were applied at $1/3$ and $2/3$ of the length of the plate using a hand operated hydraulic test system (Enerpac). Data from the SECs were acquired using an off-the-shelf DAQ (ACAM PCap01). Data from the RSGs were acquired using Hewlett-Packard 3852 DAQ.

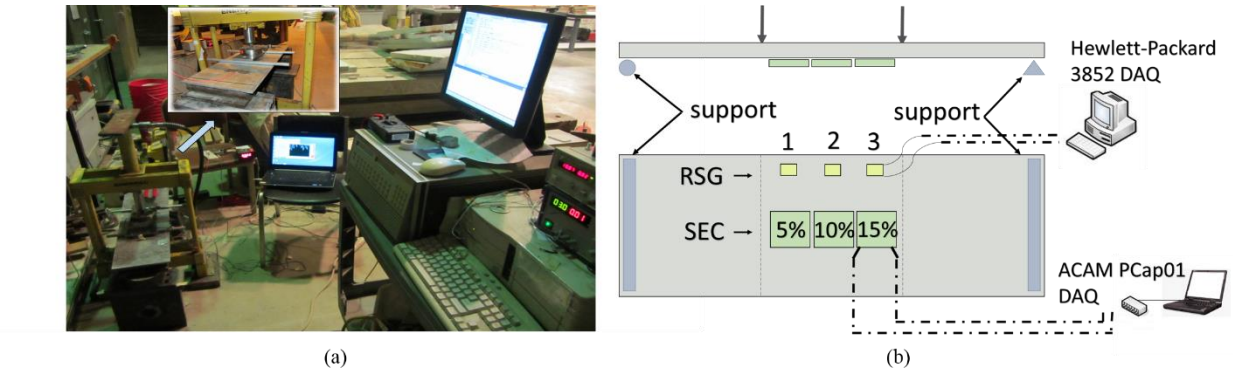

Figure 9. (a) Bending plate test laboratory setup; (b) schematic from side and under the plate (connection sensors-DAQ only shown for 2 sensors for clarity

4.2.2 Results

Figures 10 and 11 show the results for the free-standing tests. Figure 10 compares time series of strain input and capacitance measurements. Time axes of strain and capacitance were manually aligned given the inaccurate synchronization of both DAQs. The comparison of time series measurements shows an agreement between the experimental values of strain and measured capacitance. There is an upwards slope in the capacitance measurements that becomes significant at high levels of strain. This slope is attributed to the viscoelastic behavior of the nanocomposite

Figure 11 is a plot of the normalized change in capacitance versus strain. Normalized measurements provide a better comparison given that equation (7) does not hold in a free-standing configuration. Data are fitted linearly using a least square estimator. Results show that the sensor remains linear of the range 0-6% strain.

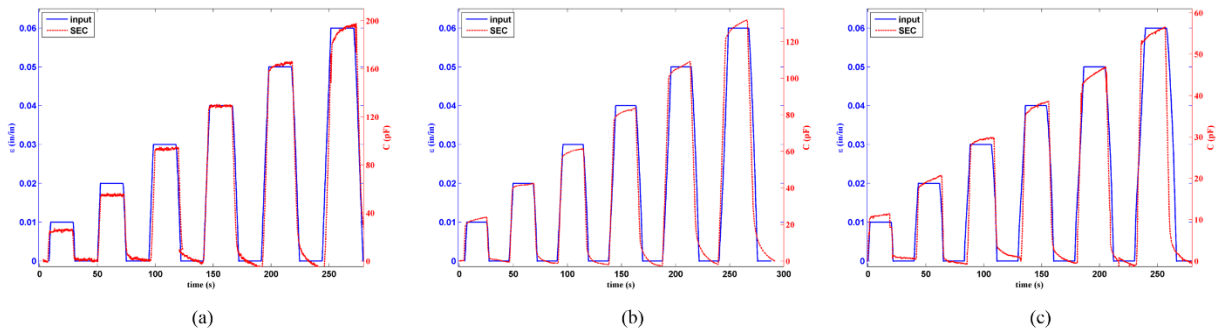

Figure 10. Strain history of SEC versus Instron RSG (free-standing test). (a) 5% TiO_2 content; (b) 10% TiO_2 content; (c) 15% TiO_2 content.

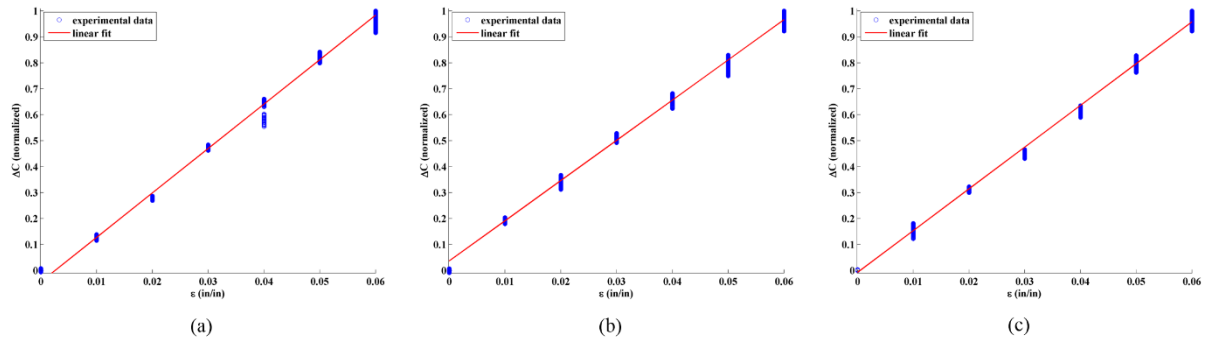

Figure 11. Verification of Linearity for free-standing bio-based SECs. (a) 5% TiO2 content; (b) 10% TiO2 content; (c) 15% TiO2 content.

Figures 12 and 13 shows the results for the bending beam test. Comparison of time series data (Figure 12) also shows agreement between strain load and measured capacitance. A noticeable feature in the signals is a drift of the signal after each step load. We hypothesize that this drift is caused by the epoxy interface, which results in a slow relaxation process of the dielectric following a load step. The experimental gauge factor is obtained by plotting $\Delta C/C$ versus strain and taking the slope of the linear fit (Figure 13). Considering a value of $\nu_m = 0.33$ for aluminium and $\nu = 0.45$-0.5 for thermosets, the theoretical gauge factor of the castor oil-based SEC is $1.34 < \lambda < 1.49$ (equation (7)). Table I summarizes the values obtained in Figure 13. The experimental gauge factors are all comprised within 1.34 and 1.49. Cross-specimens fluctuation can be

explained by slight imperfections in the dispersion of the TiO_2, and changes in environmental conditions (temperature and humidity).

Table I. Strain gauge factors of SEC installed on an aluminium plate

	5%	10%	15%
Gauge factor λ	1.415	1.376	1.463

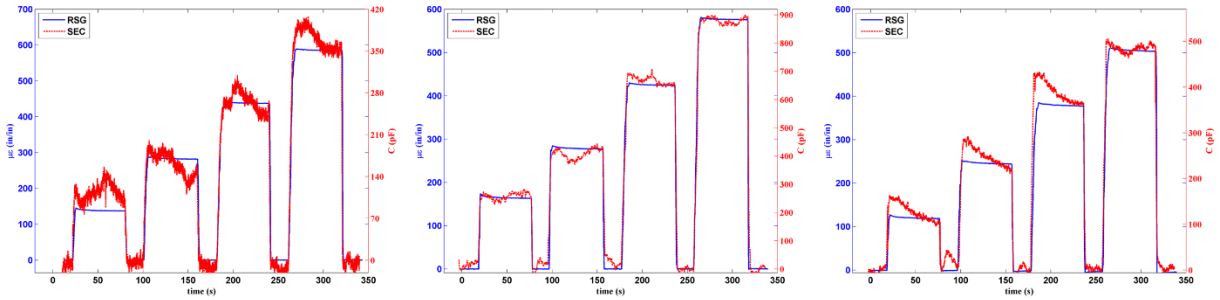

Figure 12. Strain history of SEC versus RSG (bending plate test). (a) 5% TiO2 content; (b) 10% TiO2 content; (c) 15% TiO2 content.

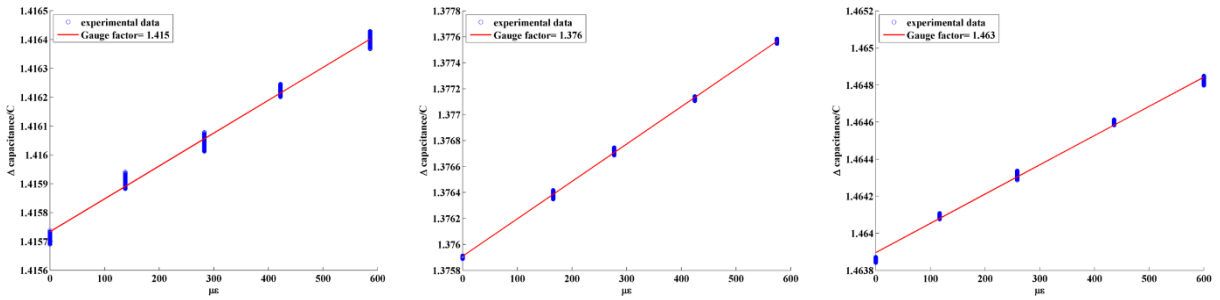

Figure 13. Verification of gauge factor for bio-based SEC (bending plate test). (a) 5% TiO2 content; (b) 10% TiO2 content; (c) 15% TiO2 content.

CHAPTER 5

CONCLUSION

This chapter is a short version of the work published in the Structural Health Monitoring journal by the author (Kharroub, 2014).

In this thesis, an inexpensive and bio-renewable material was presented to reduce the environmental footprint of large area electronics. The proposed application is an SEC, constituted from a dielectric made of castor oil-based PU filled with titanium dioxide, and conductive plates made of SEBS filled with carbon black. Such sensor could be deployed in a large network configuration to cover large-scale surfaces, enabling monitoring of local strain over global areas.

The sensor showed to reach stability after approximately 16 days from fabrication. Scanning electron microscopy tests showed that all concentrations of TiO_2 (5%, 10%, and 15%) are dispersed well in the horizontal axis, but appear to have settled in the vertical axis. The thermogravimetric analysis showed good physical and chemical properties.

Static load tests were conducted on free-standing specimens and on specimens adhered onto an aluminium plate subjected to bending. Results from free-standing specimens showed that the sensor remained linear of the range 0-6% strain, and bending tests verified the theoretical gauge factor experimentally. These results confirmed the good dispersion of the particles within the castor oil PU and that the SEC can be used as a strain sensor.

The proposed castor oil-based SEC constitutes a promising sensor for monitoring of mesoscale surfaces. It demonstrates the utilization of bio-based polymers in the fabrication of sensors, which can result in important environmental benefits. Future work include improving

the dispersion of the filler in the dielectric and adding a coupling agent to replace the SEBS with castor oil in the electrodes.

CHAPTER 6

BIOBLIOGRAPHY

1. Madbouly, S. A., Xia, Y., & Kessler, M. R. (2013). Rheological behavior of environmentally friendly castor oil-based waterborne polyurethane dispersions.*Macromolecules*, *46*(11), 4606-4616.

2. Xia, Y., & Larock, R. C. (2010). Vegetable oil-based polymeric materials: synthesis, properties, and applications. *Green Chemistry*, *12*(11), 1893-1909.
Blitz, J., & Simpson, G. (1996). *Ultrasonic methods of non-destructive testing*(Vol. 2). Springer.

3. Chiellini, E.; Cinelli, P.; Corti, A. Developments and Future Trends for Environmentally Dregradable Plastics. In Renewable Resources and Renewable Energy: A Global Challenge; Graziani, M., Fornasiero, P., Eds.; CRC Press: Boca Raton, FL, 2007; pp 63-112.

4. Laflamme, S., Kollosche, M., Connor, J. J., & Kofod, G. (2012). Soft capacitive sensor for structural health monitoring of large-scale systems. *Structural Control and Health Monitoring*, *19*(1), 70-81.

5. Laflamme, S., Saleem, H. S., Vasan, B. K., Geiger, R. L., Chen, D., Kessler, M. R., & Rajan, K. (2013). Soft Elastomeric Capacitor Network for Strain Sensing Over Large Surfaces, IEEE Trans. Mechatronics, 18(6), 1647-1654.

6. Kharroub, S., Laflamme, S., Madbouly, S., and Ubertini, F., *Bio-based Soft Elastomeric Capacitor for Structural Health Monitoring Applications*, Structural Health Monitoring (in press).

7. Blitz, J., & Simpson, G. (1996). *Ultrasonic methods of non-destructive testing*(Vol. 2). Springer.

8. Grosse, C. U. (2008). *Acoustic emission testing* (pp. 3-18). Heidelberg: Springer.

9. Rens, K. L., Wipf, T. J., & Klaiber, F. W. (1997). Review of nondestructive evaluation techniques of civil infrastructure. *Journal of performance of constructed facilities*, *11*(4), 152-160.

10. Li, H. N., Li, D. S., & Song, G. B. (2004). Recent applications of fiber optic sensors to health monitoring in civil engineering. *Engineering structures*, *26*(11), 1647-1657.

11. López-Higuera, J. M., Rodriguez Cobo, L., Quintela Incera, A., & Cobo, A. (2011). Fiber optic sensors in structural health monitoring. *Lightwave Technology, Journal of*, *29*(4), 587-608.

12. Glisic, B., & Yao, Y. (2012). Fiber optic method for health assessment of pipelines subjected to earthquake-induced ground movement. *Structural Health Monitoring*.

13. Giurgiutiu, Victor. *Structural health monitoring: with piezoelectric wafer active sensors*. Academic Press, 2007.

14. Da Costa Antunes, Paulo Fernando, et al. "Optical fiber accelerometer system for structural dynamic monitoring." *Sensors Journal, IEEE* 9.11 (2009): 1347-1354."

15. Hurlebaus, S., & Gaul, L. (2004). Smart layer for damage diagnostics. *Journal of intelligent material systems and structures*, *15*(9-10), 729-736.

16. Carlson, J. A., English, J. M., & Coe, D. J. (2006). A flexible, self-healing sensor skin. *Smart materials and structures*, *15*(5), N129.

17. Tata, U., Deshmukh, S., Chiao, J. C., Carter, R., & Huang, H. (2009). Bio-inspired sensor skins for structural health monitoring. *Smart Materials and Structures*, *18*(10), 104026.

18. Lipomi, D. J., Vosgueritchian, M., Tee, B. C., Hellstrom, S. L., Lee, J. A., Fox, C. H., & Bao, Z. (2011). Skin-like pressure and strain sensors based on transparent elastic films of carbon nanotubes. *Nature nanotechnology*, *6*(12), 788-792.

19. Hu, Y., Rieutort-Louis, W. S., Sanz-Robinson, J., Huang, L., Glisic, B., Sturm, J. C.,Wagner,S., & Verma, N. (2014). Large-scale sensing system combining large-area electronics and CMOS ICs for structural-health monitoring.

20. Zhou, Z., Zhang, B., Xia, K., Li, X., Yan, G., & Zhang, K. (2011). Smart film for crack monitoring of concrete bridges. *Structural Health Monitoring*, *10*(3), 275-289.

21. Gangopadhyay, R., & De, A. (2000). Conducting polymer nanocomposites: a brief overview. *Chemistry of Materials*, *12*(3), 608-622.

22. Loh, K. J., Hou, T. C., Lynch, J. P., & Kotov, N. A. (2009). Carbon nanotube sensing skins for spatial strain and impact damage identification. *Journal of Nondestructive Evaluation*, *28*(1), 9-25.

23. Gao, L., Thostenson, E. T., Zhang, Z., Byun, J. H., & Chou, T. W. (2010). Damage monitoring in fiber-reinforced composites under fatigue loading using carbon nanotube networks. *Philosophical Magazine*, *90*(31-32), 4085-4099.

24. Kang, I., Schulz, M. J., Kim, J. H., Shanov, V., & Shi, D. (2006). A carbon nanotube strain sensor for structural health monitoring. *Smart materials and structures*, *15*(3), 737.

25. Arshak, K. I., McDonagh, D., & Durcan, M. A. (2000). Development of new capacitive strain sensors based on thick film polymer and cermet technologies.*Sensors and Actuators A: Physical*, *79*(2), 102-114.

26. Suster, M., Guo, J., Chaimanonart, N., Ko, W. H., & Young, D. J. (2006). A high-performance MEMS capacitive strain sensing system.*Microelectromechanical Systems, Journal of*, *15*(5), 1069-1077.

27. Dobrzynska, J. A., & Gijs, M. A. M. (2013). Polymer-based flexible capacitive sensor for three-axial force measurements. *Journal of Micromechanics and Microengineering*, *23*(1), 015009.

28. Harrey, P. M., Ramsey, B. J., Evans, P. S. A., & Harrison, D. J. (2002). Capacitive-type humidity sensors fabricated using the offset lithographic printing process. *Sensors and Actuators B: Chemical*, *87*(2), 226-232.

29. Hong, H. P., Jung, K. H., Min, N. K., Rhee, Y. H., & Park, C. W. (2012). A highly fast capacitive-type humidity sensor using percolating carbon nanotube films as a porous electrode material. *Proc. IEEE Sensors (Taipei, Oct. 2012)*, 1-4.

30. Lu, Y., & Larock, R. C. (2008). Soybean-oil-based waterborne polyurethane dispersions: effects of polyol functionality and hard segment content on properties. *Biomacromolecules*, *9*(11), 3332-3340.

31. Lu, Y., Tighzert, L., Dole, P., & Erre, D. (2005). Preparation and properties of starch thermoplastics modified with waterborne polyurethane from renewable resources. *Polymer*, *46*(23), 9863-9870.

32. Yang, D., Tian, M., Dong, Y., Kang, H., Gong, D., & Zhang, L. (2013). A high-performance dielectric elastomer consisting of bio-based polyester elastomer and titanium dioxide powder. *Journal of Applied Physics*, *114*(15), 154104.

33. Laflamme, S., Kollosche, M., Connor, J. J., & Kofod, G. (2012). Robust flexible capacitive surface sensor for structural health monitoring applications. *Journal of Engineering Mechanics*, *139*(7), 879-885.

34. Saleem, H., M. Thunga, M. Kollosche, M. R. Kessler, and S. Laflamme. "Interfacial treatment effects on behavior of soft nano-composites for highly stretchable dielectrics." *Polymer* 55, no. 17 (2014): 4531-4537.